



LAWRENCE
LIVERMORE
NATIONAL
LABORATORY

Molecular Dynamics Simulations of Spinodal-Assisted Polymer Crystallization

R. H. Gee, N. M. Lacevic, L. Fried

July 11, 2005

International Conference of Computational Methods in
Sciences and Engineering
Loutraki, Greece
October 21, 2005 through October 26, 2005

Disclaimer

This document was prepared as an account of work sponsored by an agency of the United States Government. Neither the United States Government nor the University of California nor any of their employees, makes any warranty, express or implied, or assumes any legal liability or responsibility for the accuracy, completeness, or usefulness of any information, apparatus, product, or process disclosed, or represents that its use would not infringe privately owned rights. Reference herein to any specific commercial product, process, or service by trade name, trademark, manufacturer, or otherwise, does not necessarily constitute or imply its endorsement, recommendation, or favoring by the United States Government or the University of California. The views and opinions of authors expressed herein do not necessarily state or reflect those of the United States Government or the University of California, and shall not be used for advertising or product endorsement purposes.

Molecular Dynamics Simulations of Spinodal-Assisted Polymer Crystallization

Richard H. Gee¹, Naida M. Lacevic, and Larry E. Fried

Chemistry and Materials Science Directorate
Laurence Livermore National Laboratory
P.O. Box 808, L-268, Livermore, CA 94550

Received 8 July, 2005; accepted in revised form X July, 2005

Abstract: Large scale molecular dynamics simulations of bulk melts of polar (poly(vinylidene fluoride) (pVDF)) polymers are utilized to study chain conformation and ordering prior to crystallization under cooling. While the late stages of polymer crystallization have been studied in great detail, recent theoretical and experimental evidence indicates that there are important phenomena occurring in the early stages of polymer crystallization that are not understood to the same degree. When the polymer melt is quenched from a temperature above the melting temperature to the crystallization temperature, crystallization does not occur instantaneously. This initial interval without crystalline order is characterized as an induction period. It has been thought of as a nucleation period in the classical theories of polymer crystallization, but recent experiments,¹ computer simulations,² and theoretical work³ suggest that the initial period in polymer crystallization is assisted by a spinodal decomposition type mechanism. In this study we have achieved physically realistic length scales to study early stages of polymer ordering, and show that spinodal-assisted ordering prior to crystallization is operative in polar polymers suggesting general applicability of this process.

Keywords: poly(vinylidene fluoride), polymer crystallization, early stages, molecular dynamics

Subject Classification: Polymer Physics

PACS: 61.41.+e, 81.05.Kf

1. Introduction

One of the most challenging problems in polymer physics is understanding the dynamics and thermodynamics of polymer crystallization. When the polymer melt is quenched from a temperature above the melting temperature to the crystallization temperature, crystallization does not occur instantaneously. This interval without crystalline order is characterized as an induction period. Imai and coworkers performed a detailed investigation of this induction period via small angle x-ray scattering (SAXS) experiments of poly(ethylene terephthalate) (PET). They have shown that density fluctuations occur in the induction period. Inspired by the work of Imai,⁴ Olmstead and coworkers³ proposed a generalized phase diagram that describes the polymer crystallization from the melt. This phase diagram suggests that there are three types of primary nucleation: direct, binodal and spinodal.¹

In this study we focus on the spinodal-type primary nucleation. The observation of an induction period in experiments is highly dependent on the sensitivity of the detector,⁵ therefore molecular dynamics (MD) simulations are an excellent tool to probe the length scales of this process. Increased computational power has helped to achieve realistic length scales in molecular dynamics simulations that are necessary to probe the early stages of primary nucleation⁶ and test theoretical predictions.³

The purpose of this study is to demonstrate general applicability of spinodal-type primary nucleation prior to crystallization via simulations and to obtain physical insight in polymer ordering prior to crystallization upon deep quench.

2. Computational Methods

2.1 pVDF Melt Representation and Force Fields

MD simulations of the polymer melts were carried out on bulk entangled amorphous ensembles of both explicit atom (EA) and united-atom (UA) linear polymers. The simplified UA model affords the investigation of a much larger polymer ensemble as compared to explicit atom representations, thus allowing one to resolve the important SAXS peaks identifiable experimentally. The polymer melt is composed of either ten 120-mer polymer (240 backbone carbons) EA chains (7,220 explicit-atoms; $M_w=7,682$ g/mol), or 8,640 240-bead polymer chains (2,073,600 united-atoms; $M_w=7,682$ g/mol). The polymer models are representative of poly(vinylidene fluoride) (pVDF). In the UA polymer models, the hydrogen or fluorine atoms are lumped onto the carbon backbone atoms to which they are attached. The EA simulations employed the COMPASS¹⁹ force field parameter set, while the UA simulations employed the force field parameter set of Goddard *et al.*^{8,9} The force field parameters consist of both valence (stretch, bending, and torsion terms) and non-bonded potential terms (vdW and Coulomb). All valence degrees of freedom were explicitly treated and unimpeded.

2.2 Molecular Dynamics Method

Molecular dynamics is a widely used method in the investigation of various physical processes related to the dynamics of macromolecules (e.g. deformation of solids, polymer crystallization, aging in supercooled liquids, motion of biomolecules). MD provides static and dynamics properties for a collection of particles, which allow atomic scale insights that are difficult to gain otherwise.

We used three-dimensional cubic periodic boundary conditions. The simulations were carried out using constant particle number, pressure, and temperature (*NPT*) dynamics at zero pressure. All computations were carried out using the LAMMPS code.¹⁰ The particle-particle particle-mesh Ewald (PPPM) method¹⁴ was used for the treatment of long-range electrostatic interactions.

The polymer melts were initially equilibrated at a temperature well above the temperature at which ordering occurs, T_c . The periodic box was allowed to relax under *NPT* conditions for a minimum of 5 ns. Following this equilibration step, the melts were cooled in *NPT* runs in increments of 50 K and equilibrated for a minimum of 5 ns at temperatures above T_c . For the temperature at which the polymer melts order, the simulations were carried out for more than 30 ns.

3. Results and Discussions

Figure 1 demonstrates that a microphase separation from the amorphous melt into many ordered liquid domains occurs very early in the simulations for both EA and UA polymer melt models.

We next turn our attention to the process of nucleation and growth, and the question of why the pVDF forms three-dimensional ordered structures. The overall evolution of the orientationally ordered structure of pVDF is easily identified by comparing the initial starting configuration (Figure 2a) of the polymer melt to the final orientationally ordered structure (Figure 2e). The nucleation and growth process is illustrated for the ten chain 120-mer ensemble in Figure 4a-e, where snapshots of the chain conformation at various times throughout the simulation ($t = 5, 7.5, 10, \text{ and } 15 \text{ ns}$) at a temperature above T_c (panel a-c) and at a temperature at T_c (panel d-e). The melt-to-crystal phase transition occurs via an effective three stage process, consisting of first, local chain ordering, in which random sequences of the polymer backbone form small all *trans* segments on the order of two or three *trans* conformations (“*extended trans sequence formation*”), second, cluster formation, in which the randomly oriented small *trans* segments aggregate (“*cluster formation*”), and third, a stage which primarily consists of stem growth (gauche defect removal), polymer chain registration, and “lamella” thickening (“*growth*”). It is during this stage that the *trans* states become increasingly populated, and the polymer disentangles itself.

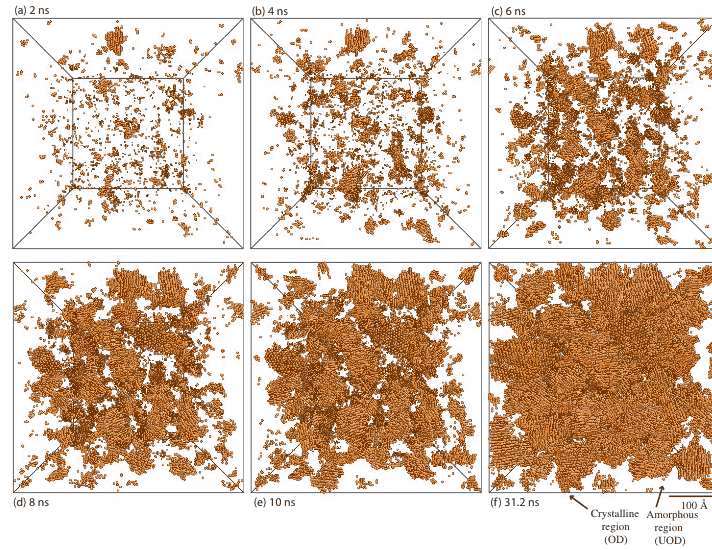


Figure 1. Snapshots from MD simulations showing the evolution of ordered domains of UA pVDF (at times of 2, 4, 6, 10, and 31.2 ns, panels (a)-(f), respectively). Only oriented domains (OD) are shown (the unordered domains (UOD) (amorphous regions) are shown in white).

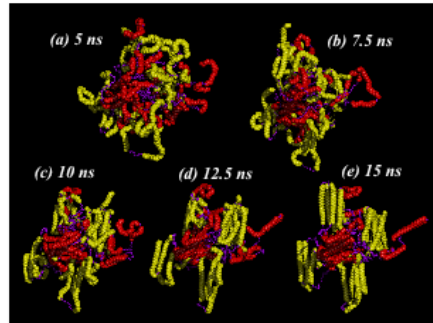


Figure 2. Illustration of the time evolution of EA pVDF ordering. (a) initial starting configuration at 50 K above T_c , (b) after 2.5 ns at 50 K above T_c , (c) after 5 ns 50 K above T_c , (d) after 2.5 ns at T_c , (e) after 5 ns at T_c . “Loops” into and out of the ordered domains and “amorphous” regions are colored purple. Only the carbon backbone atoms are shown for clarity. Chain segments colored red and yellow illustrate the polycrystalline nature of the ensemble. Time labels are for the total simulation time.

Figure 3a shows the evolution of the structure factor $S(q, t)$ for UA pVDF. $S(q, t)$ shows three distinct peaks that increase in magnitude during the simulations. Those peaks are: the induction peak, long peak and Bragg peak. Experimentally, the induction and long peak are observed via small angle x-ray scattering and the second-order Bragg peak is observed in wide angle x-ray scattering (WAXS). The induction peak is related to density fluctuations of the rigid segments. The long peak is related to alternating unordered and ordered domains. The second-order Bragg peak, which corresponds to the nearest-neighbor packing distance between polymer chains, is related to densification of the system and transition from unoriented to oriented domains.

In order to demonstrate that we observe a spinodal-assisted ordering process we calculate the growth rate $R(q)$ from $S(q, t) \propto S(q, 0) \exp[2R(q)t]$ for UA pVDF melts. $R(q)$ is a central quantity in the Cahn-Hilliard theory of spinodal decomposition,¹⁵ and according to this theory, density fluctuations grow exponentially for a liquid undergoing a demixing instability. Figure 2b shows a Cahn plot ($R(q)/q^2$ versus q^2) for UA

pVDF. The linear behavior with a negative slope observed in $R(q)$ for the polymer melts suggests that spinodal-assisted ordering prior to crystallization.

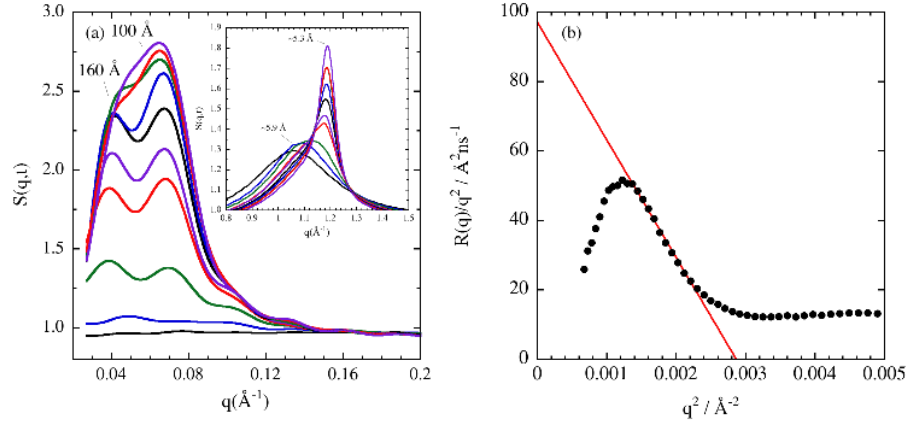


Figure 3. Evolution of the structure factor $S(q)$ for UA pVDF (panel *a*). The induction, long and Bragg peaks increase during the simulation. The induction peak merges with the long peak suggesting that spinodal-assisted ordering is completed. The inset shown the time evolution of the second-order Bragg peak. Panel *b* shows the Cahn-Hilliard plot derived from the early stages of the nucleation process in the polymer crystallization simulations for pVDF. The solid lines are a fit to the data. The linear nature of the plot demonstrates the presence of a spinodal-assisted crystallization process in undercooled polymer melts.

In order to characterize structural evolution of $S(q,t)$, we calculated the integral of $S(q,t)$ in the q -range (0.027,0.05) (integrated induction peak) and (0.05-0.1) (integrated long peak), and time evolution of the second-order Bragg peak location. Figure 4*a* shows the time dependence of the integrated induction peak and the integrated long peak for UA pVDF. The integrated induction peak grows in time until approximately 15 ns and saturates after this time, while the integrated long peak grows in time during the entire simulation. This suggests that spinodal-assisted ordering prior crystallization is completed after approximately 15 ns, and ordered domains continue to grow throughout the simulation. Figure 4*b* shows the time evolution of the second-order Bragg peak location, converted to an effective interchain distance, d . The abrupt change in d at approximately 10 ns for UA pVDF indicates a phase transition between unoriented and oriented domains.

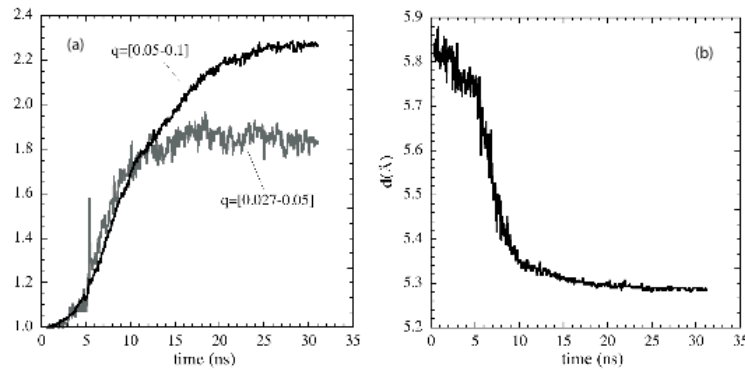


Figure 4. The time evolution of integrated intensity of the small-angle scattering peaks [$S(q,t)$ integrated for q values as labeled] are shown in for UA pVDF (panel *a*). The time evolution of the second-order Bragg peak location, converted to an effective interchain distance, d , for UA pVDF (panel *b*).

4. Conclusions

In this paper we presented a study of polar pVDF polymer melt properties upon undercooling. We find that polymer chains cooled from the melt attain critical rigid stem lengths, and illustrate the mechanism by which ordering occurs. Further, we provide evidence that ordering is a spinodal-assisted nucleation and is driven by the growth of rigid segments. The spinodal-assisted nucleation is demonstrated showing the linearity of the growth rates in the Cahn-Hilliard plots. The detailed comparison of spinodal-assisted nucleation of both polar and non-polar polymer melts will be presented elsewhere.

Acknowledgments

The work was performed under the auspices of the U.S. Department of Energy by the University of California Lawrence Livermore National Laboratory under Contract W-7405-Eng-48. We thank the Livermore Computing for generous amounts of CPU time on Thunder and MCR clusters.

References

1. Kaji, K., Nishida, K., Matsuba, G., Kanaya, T. & Imai, M. Details of Structure Formation During the Induction Period of Spinodal-Type Polymer Crystallization. *Journal of Macromolecular Science-Physics B42*, 709-715 (2003), and references therein.
2. Gee, R. H. & Fried, L. E. Ultrafast crystallization of polar polymer melts. *J. Chem. Phys.* 118, 3827 (2003), and references therein.
3. Olmsted, P. D., W.C.K.Poon, McLeish, T. C. B., Terrill, N. J. & A.J.Ryan. Spinodal-Assisted Crystallization in Polymer Melts. *Physical Review Letters* 81, 373 (1998), and references therein.
4. Imai, M., Kaji, K., Kanaya, T. & Sakai, Y. Ordering Process in the induction period of crystallization of poly(ethylene terephthalate). *Physical Review B* 52, 12696 (1995).
5. Mandelkern, L., Martin, G. M. & F.A. Juinn, J. J. *Res. Nat. Bur. Stand* 58, 2745 (1957).
6. Gee, R. H., Lacevic, N. M. & Fried, L. E. Atomistic Simulation of Spinodal-Assisted Polymer Crystallization. *Nature Materials* (in review) (2005).
7. Paul, W., Yoon, D. Y. & Smith, G. D. An optimized united atom model for simulations of polymethylene melts. *J. Chem. Phys.* 103, 1702-1709 (1995).
8. Mayo, S. L., Olafson, B. D. & Goddard, W. A. *J.Phys. Chem.* 94, 8897 (1990).
9. Gao, G. (California Institute of Technology, 1998).
10. Plimpton, S. J. Fast Parallel Algorithms for Short-Range Molecular Dynamics. *J. Comp. Phys.* 117, 1-19 (1995).
11. Verlet, L. Computer "Experiments" on Classical Fluids. I. Thermodynamical Properties of Lennard-Jones Molecules. *Phys. Rev.* 159, 98 (1967).
12. Nose, S. A unified formulation of the constant temperature molecular dynamics methods. *J. Chem. Phys.* 81, 511 (1984), and references therein.
13. Melchionna, S., Ciccotti, G. & Holian, B. L. Hoover's style Molecular Dynamics for systems varying in shape and size. *Mol. Phys.* 78, 533 (1993).
14. Hockney, R. W. & Eastwood, J. W. *Computer Simulation using Particles* (McGraw-Hill, New York, 1981).
15. Cahn, J. W. & Hilliard, J. E. Free energy of a nonuniform system I. Interfacial free energy. *J. Chem. Phys.* 28, 25 (1958).